ERDC/CRREL TR-00-21

Cold Regions Research
and Engineering Laboratory

Physical and Chemical Factors Affecting Contaminant Hydrology in Cold Environments

Steven A. Grant   December 2000

20021231 073

Abstract: This report surveys some of the physical and chemical effects of cold temperatures that should be considered when developing a contaminant-transport model. This discussion begins with a working definition of cold regions for the purpose of contaminant hydrology modeling: an area with appreciable frozen ground and with a substantial fraction of the annual precipitation falling as snow. The chemical thermodynamics of geochemical solutions below 0°C is then reviewed. Particular attention is placed on the physical–chemical properties of ice and liquid water at subzero temperatures. Finally, models that estimate the liquid water content and hydraulic conductivity of frozen ground are discussed.

Technical Report
ERDC/CRREL TR-00-21

**US Army Corps
of Engineers®**
Cold Regions Research &
Engineering Laboratory

Physical and Chemical Factors Affecting Contaminant Hydrology in Cold Environments

Steven A. Grant   December 2000

PREFACE

CONTENTS

ILLUSTRATIONS

Figure

TABLE

Table

NOMENCLATURE

Symbol	Definition	SI unit	Eq. first cited
a_B	activity of B	dimensionless	28
A_0	parameter in modified Vand equation	$dm^3\,mol^{-1}$	7
A_1	parameter in modified Vand equation	$dm^3\,mol^{-1}\,K^{-1}$	7
A_3	fitted parameter in Vand equation	$dm^3\,mol^{-1}$	7
B	parameter in VTF equation		5
B_1, B_2, B_3	parameters in modified VTF equation		6
$B_X^{(n)}$	parameter in Speedy's equation		3
$B_\alpha^{(n)}$	parameter in Speedy's equation		4
c	solute concentration	$mol\,dm^{-3}$	
c_j	aqueous concentration of the jth solute	$mol\,m^{-3}$	2
C_p	isobaric heat capacity	$J\,mol^{-1}$	10
C_X	parameter in Speedy's equation		3
C_α	parameter in Speedy's equation		4
$\mathbf{D}$	dispersivity tensor	$m^2\,s^{-1}$	2
f	parameter in empirical equation	$m\,°C^{-1}$	text
f_B	rational activity coefficient	dimensionless	31
g	acceleration due to gravity	$m\,s^{-2}$	1
G	Gibbs energy	J	24
G_T	total Gibbs energy of a mixture or solution	J	23
$\overline{G}_A$	partial molar Gibbs energy of component A	$J\,mol^{-1}$	24
h	total head	Pa	1
$\mathbf{k}$	permeability tensor	m^2	1
$\mathbf{K}$	hydraulic conductivity tensor	$m^2\,Pa^{-1}\,s^{-1}$	1
K_f	cryoscopic constant	$K\,mol^{-1}$	48
m_B	molality B	$mol\,kg^{-1}$	30
M_A	molecular mass of solvent A	$kg\,mol^{-1}$	30
n_A	amount of component A in a mixture or solution	mol	20
n_T	total number of molecules in a mixture	mol	20
p	pressure	Pa	11
p_c	capillary pressure	Pa	11
p_i	pressure gradient across ice/liquid/water interface in water-saturated porous media	Pa	11
p_{rc}	conventional reference pressure	Pa	11
p_{rw}	working reference pressure for supercooled water	Pa	11
Q'	fitted parameter in Vand equation	$mol\,dm^3\,mol^{-1}$	7

Symbol	Definition	SI unit	Eq. first cited
Q'_0	fitted parameter in modified Vand equation	mol dm^3 mol^{-1}	8
Q'_1	fitted parameter in modified Vand equation	mol dm^3 mol^{-1} K^{-1}	8
Q_{c_j}	a source-sink term for the jth solute	mol m^{-3} s^{-1}	2
r	mean radius of largest undrained pore class	m	54
$\overline{S}_m^{\alpha}$	molar entropy of the α phase	J K^{-1} mol^{-1}	13
t	temperature ($\equiv T - 273.15$)	°C	5
t_0	parameter in VTF equation = 123.15°C	°C	5
T	thermodynamic temperature	K	3
T^{s+l}	freezing temperature of a solution	K	43
$T^{s+l,*}$	freezing temperature of a pure solvent	K	43
T_{rc}	conventional reference temperature = 298.15 K	K	11
T_{rw}	working reference temperature = 273.15 K	K	11
T_s	limiting temperature for supercooled water = 227.15 K	K	3
$\mathbf{v}$	Darcian flow velocity vector	m s^{-1}	1
V_m^{α}	molar volume of the α phase	m^3	51
V_T	total volume of a system	m^3	21
$\overline{V}_A$	partial molar volume of component A	m^3 mol^{-1}	22
x_B^{α}	mole fraction of B in the α phase	dimensionless	29
X	a physical property of supercooled water		3
z	vertical distance above datum	m	1
α	parameter in van Genuchten equation	m^{-1}	83
γ_{iw}	interfacial tension of ice against water	N m^{-1}	78
γ_{wa}	interfacial tension of water against air	N m^{-1}	9
γ_B	activity coefficient for solute B	kg mol^{-1}	32
$\gamma_{\pm BC}$	mean-ionic activity coefficient for solute BC	dimensionless	39
$\Delta_s^l H_m^*$	molar enthalpy of melting for pure water	J mol^{-1}	14
ΔT	depression of solvent freezing point = $(T^{s+l,*} - T^{s+l})$	K	47
ε	reduced temperature $\equiv (T - T_s)/T_s$	dimensionless	3
θ	volumetric liquid-water content	dimensionless	53
θ_r	residual liquid-water content	dimensionless	84
θ_s	saturated liquid-water content	dimensionless	84
Θ	reduced liquid-water content	dimensionless	83
λ	parameter in van Genuchten equation	dimensionless	83
μ_B	chemical potential of B	J mol^{-1}	27
$\mu_B^{\ominus}$	standard state chemical potential of B	J mol^{-1}	28
μ_B^{α}	chemical potential of B in the α phase	J mol^{-1}	58
ν	viscosity	Pa s	5
ν_0	reference viscosity in VTF equation	Pa s	5

vi

Symbol	Definition	SI unit	*Eq. first cited*
v_{rel}	relative viscosity in Vand equation	Pa s	5
ρ	density	kg m^{-3}	4
ρ_s	reference density	kg m^{-3}	4
Φ	porosity	dimensionless	2
ϕ	air–water contact angle at solid	rad	54
Ψ	matric potential	m	53
Ψ_i	p_i expressed in terms of height of liquid water	m	78
$-$	overbar symbol indicates a molar quantity		12
Θ	superscript indicating a standard substance		28
*	superscript indicating a pure substance		11

Physical and Chemical Factors Affecting Contaminant Hydrology in Cold Environments

STEVEN A. GRANT

INTRODUCTION

Definition of cold regions

Lexically, the adjective "cold" refers to an environment in which the ambient temperature is noticeably below body temperature. A cold region is one in which lower temperatures have significant effects on the natural environment or human activities. While moderate temperatures may be perceived as "cold," cold regions have been typically defined by the intervals in which ambient temperatures are below the melting temperature of water, because it is at these temperatures that the effects of cold temperatures are most pronounced. Among the criteria that have been used to delineate cold regions are (Bates and Bilello 1966)

1. Air temperatures below 0°C or –18°C (32°F and 0°F, respectively) that had a 50% likelihood of being observed annually
2. Mean annual snow depth
3. Ice cover on navigable rivers
4. Isolines based on permanence, depth, and continuity of frozen ground.

Traditionally, the maps made from plotting isograms based on these criteria delineate the changes in human activities due to cold. For example, isograms based on frozen ground delineate changes in the construction requirements for building footings. Isograms based on ice cover speak to the navigability of the waters during some portion of the year.

This report discusses how cold temperatures affect contaminant-transport modeling; cold regions should be delineated by the cold-regions phenomena necessary to make the model a valid representation of the pertinent chemical, physical, and microbiological processes that determine the fate of contaminants in the environment. Cold temperatures affect the physics of contaminant transport by freezing the water in the ground (sometimes to great depths) and by blanketing the ground (seasonally or permanently) with snow. Since no maps have been drawn delineating the cold-regions effects on contaminant hydrology, the natural delineations would be those for snow covers and extents of ground freezing.

Extent of cold regions

In comparing the hydrologic systems of cold regions with those of warmer areas, two factors distinguish the former systems:

1. Some of the annual precipitation occurs as snow, which completes its role in the hydrologic cycle during a comparatively brief period as snowmelt.
2. The ground freezes to some depth. Ground freezing reduces the soil's permeability and its water-storage capacity. Accordingly, ground freezing dramatically decreases the soil's infiltration rate and just as dramatically increases run-off from the soil of water from rain and snowmelt.
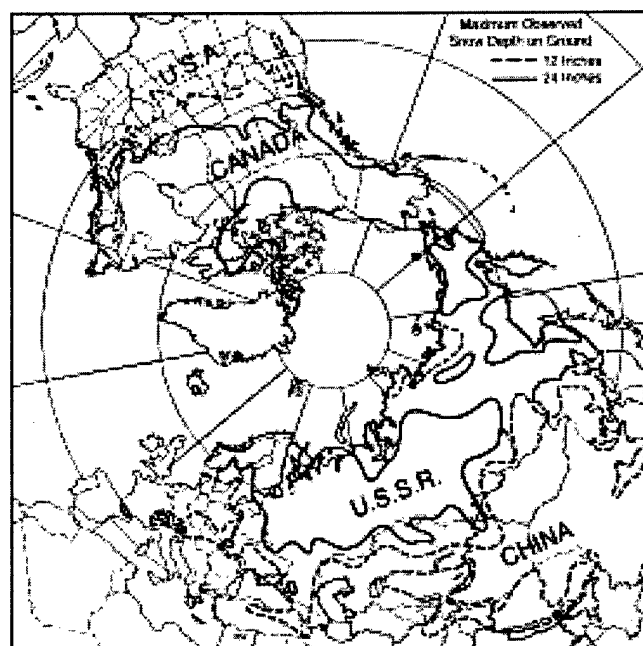
Figure 1. Cold-regions boundaries as determined by snow depths. (From Bates and Bilello 1966.)

To be hydrologically important, a cold region must receive an appreciable proportion of its precipitation as snow, and its ground must be frozen so that the infiltration of the melting snow is limited. In the northern hemisphere, these two criteria can be applied to delineate the extent of cold regions for the purposes of contaminant-transport modeling.

Snow cover

Bates and Bilello (1966) developed maps with isograms of various annual snow depths (Fig. 1).

Much of the United States has average annual snow depths of 0.3 m (12 in.) or more. This includes all or part of the following states: Alaska, California, Connecticut, Idaho, Illinois, Indiana, Massachusetts, Maine, Michigan, Minnesota, Missouri, Montana, Nebraska, Nevada, New Hampshire, New Jersey, New York, North Dakota, Ohio, Pennsylvania, South Dakota, Utah, Vermont, Washington, Wisconsin, and Wyoming. The isogram in Figure 1 indicates the annual quantity, but not the annual fraction, of precipitation that typically arrives as snow and, therefore, does not indicate the relative importance of snow to a region's hydrology. Accordingly, the isogram in Figure 1 may not adequately delineate snow-affected areas in drier regions.

Frozen ground

Three major classes of frozen ground are recognized: seasonally frozen ground, discontinuous permafrost, and permafrost.

Seasonally frozen ground. The potential inadequacy of snow-depth isograms to delineate cold, dry areas is borne out by the map of permafrost and frost-affected areas (Fig. 2), also by Bates and Bilello (1966). Understandably, the southernmost isogram, that for frost penetration, is similar to that for snow cover. However, several areas (mostly in the western United States) with low rates of annual precipitation are now included. These areas are all or parts of Arizona, Colorado, Kansas, Maryland, Missouri, New Mexico, and Rhode Island.

Discontinuous permafrost. In the United States, discontinuous permafrost is found only in

2
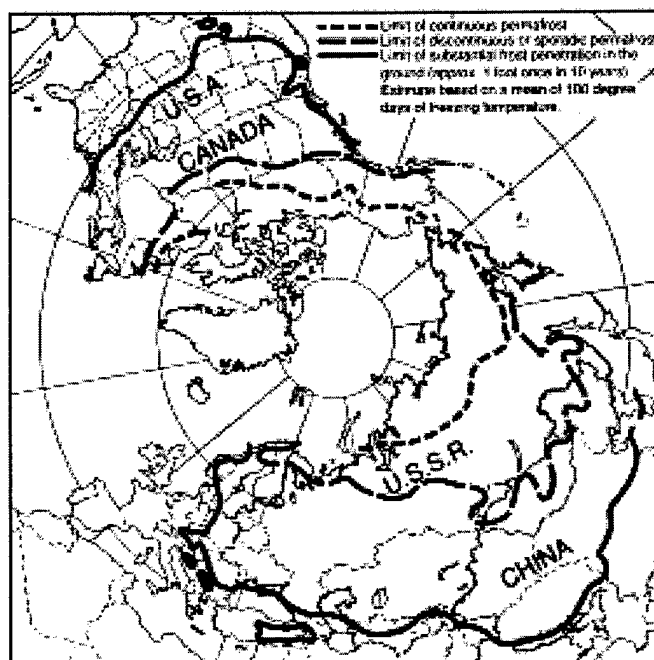
Figure 2. Cold-regions boundaries as determined by frozen ground. (From Bates and Bilello 1966.)

Alaska. Discontinuous permafrost or permafrost is found under most of the land surface of that state.

Permafrost. Areas of permafrost, in which no seasonally thawed land occurs, are found in the northernmost parts of Alaska.

Importance to contaminant-transport modeling

A model is a mathematical expression of the developer's understanding of the system being simulated. Accordingly, contaminant-transport models valid for cold regions differ from those appropriate for warmer climates because the system being described is conspicuously different. The following modeling aspects differentiate contaminant-transport models valid in cold regions:

1. Much of what is understood about the hydrology of cold regions is qualitative. Because there have been comparatively few studies in cold regions, the physical, chemical, and biological processes that determine the contaminant hydrology of cold regions are not completely understood. This lack of quantitative knowledge hinders the development of physically based contaminant-transport models valid for cold regions. Much basic research is needed to support the development of simulation models that are appropriate for these regions.

2. The energy flow and aqueous-solution phase transitions must be included explicitly in the development of solute transport models.

3. In unfrozen porous media, liquid water moves largely in response to hydrostatic gradients. In frozen porous media, liquid water movement in response to osmotic or thermal gradients may be dominant.

4. The physical chemistry of electrolyte solutions in natural porous media above freezing temperatures is well understood, and models describing them are generally available. For systems below 0°C, there are comparatively few physical chemical data (aside from freezing-point depression determinations) for even simple electrolyte solutions.

3

5. Much of the groundwater in areas with permafrost is brackish and impotable. Unlucky contamination of currently exploited aquifers that are potable can effectively deprive communities of potable subterranean water supplies.

How these effects are incorporated in mathematical models of contaminant transport can be outlined with the differential equations that form the basis of many of these models. Water in a porous medium flows in a linearly proportional response to the hydrostatic gradient across that medium. This observation has been formalized as Darcy's law, the vector form of which is

$$\mathbf{v} = -\frac{\mathbf{k}}{v} \bullet (\nabla p - \rho g \nabla z) = -\mathbf{K} \bullet \nabla h \qquad (1)$$

where $\mathbf{v}$ = Darcian flow velocity vector (m s^{-1})
$\quad \mathbf{k}$ = permeability tensor (m^2)
$\quad v$ = viscosity of fluid (Pa s)
$\quad p$ = fluid pressure (Pa)
$\quad \rho$ = fluid density (kg m^{-3})
$\quad g$ = acceleration due to gravity (m s^{-2})
$\quad z$ = vertical distance above datum (m)
$\quad \mathbf{K}$ = hydraulic conductivity tensor, which in this treatment is assigned dimensions of m^2 Pa^{-1} s^{-1}
$\quad h$ = total head (Pa).

(The formulas presented here are from Mangold and Tsang [1991].) As will be discussed in later sections, cold temperatures dramatically affect three of the parameters in eq 1: v, p, and $\mathbf{K}$. The viscosity of the aqueous solution in freezing soils is affected directly by lowering temperatures, which cause the viscosity of pure water to increase by an order of magnitude, and by solutes excluded from ice forming in the soil solution, which cause the viscosity of the remaining liquid-water solution to be increased still further. The pressure of vicinal water in frozen porous media is controversial and an active area of basic research (Zheng et al. 1991). It is clear that the liquid-pressure gradients accompanying differences in temperature may be much more important than pressure gradients due to elevation or water content (see, for example, Perfect et al. [1991]). Finally, as ice occupies some of the pore space, the conductivity of the porous material is reduced.

Once the flow of water is established, the more challenging problem of solute flows through porous media can be addressed. In many cases, the appropriate partial differential equation to describe the transport of the solute j is

$$\nabla \bullet \left(\mathbf{v} c_j \right) - \nabla \bullet \left(\mathbf{D} \bullet \nabla c_j \right) = \frac{\partial}{\partial t} \Phi \, c_j + Q c_j \qquad (2)$$

where c_j = aqueous concentration of jth solute (mol m^{-3})
$\quad \mathbf{D}$ = dispersivity tensor (m^2 s^{-1})
$\quad \Phi$ = porosity of porous medium (dimensionless)
$\quad Q c_j$ = source-sink term for jth solute (mol m^{-3} s^{-1}).

As would be expected, most of the geochemical reactions that contribute to the terms $Q c_j$ are affected by temperature. The most pronounced of these effects are on the chemical–thermodynamic state of the solutes and consequently on their solubility, miscibility, speciation, and reactivity.

AQUATIC CHEMISTRY BELOW 0°C

The transport of solutes and non-aqueous-phase liquids in any porous medium, frozen or unfrozen, is directly affected by the physical–chemical properties of the solvents and solutes in the system. These properties can be measured, but in many cases the careful

4

application of chemical–thermodynamic information can spare the modeler from making many tedious measurements in the laboratory. While few systems have been studied as extensively as aqueous systems, there is a paucity of data at subzero temperatures. This section discusses the physical–chemical properties of the solvent, water, as a pure liquid. After a brief discussion of the relevant chemical thermodynamics, the section concludes with a discussion of the properties of aqueous solutions at subzero temperatures.

Physical properties of liquid water

The state and movement of water in frozen and unfrozen ground is affected by several of its physical properties, all of which change with temperature to some degree. Some of these temperature effects are trivial, but others must be taken into account explicitly when modeling solute transport.

The most up-to-date tabulations of the physical–chemical properties of liquid water have been presented in the *Journal of Physical and Chemical Reference Data* (a recent cumulative index is presented on page 1368 of volume 20). Many of these properties can be modeled conveniently with the numerical equation-of-state package developed by Hill (1990).

Most of the physical properties of supercooled water have been measured to roughly –35°C. The temperature trends of these physical properties are consistent with a limiting behavior for many physical properties of liquid water at a unique temperature, apparently –46°C. Speedy (1987) fitted three properties of supercooled water—cubic expansion coefficient (α), isothermal compressibility (κ_T), and heat capacity at constant pressure (C_p)—to an empirical relation:

$$X = \sum_{n=0} B_X^{(n)} \varepsilon^n + 2C_X \varepsilon^{-1/2} , \qquad (3)$$

where X is the physical property being described. The empirical coefficients B_X and C_X have been fitted to the model from experimental data. The parameter ε is a reduced temperature [$= (T - T_s)/T_s$], T_s being a limiting temperature that is assumed to be exactly 227.15 K (–46°C). The fitted parameters of the Speedy model are presented in Table 1.

Table 1. Coefficients to Speedy's (1987) empirical equation for calculating heat capacity, thermal expansivity, compressibility, and viscosity of supercooled water.

Parameter	Cubic expansion coefficient $\alpha \times 10^3$ (K)	Isothermal compressibility κ_T (bar^{-1})	Heat capacity at constant pressure C_p (J K^{-1} mol^{-1})	Viscosity ν (Pa s^{-1})
C_X	–0.80	20.0	14.2	26.312
$B_X^{(0)}$	1.802 180 3	4.120	24.952	–144.565
$B_X^{(1)}$	–0.941 698 0	–1.130	128.281	1,239.075
$B_X^{(2)}$	0.905 507 0	77.817	14.2	–8,352.579
$B_X^{(3)}$	–0.80	–78.143	–221.405	31,430.760
$B_X^{(4)}$		54.290	–64.812	–48,576.798
Max resid	1.2 ppm	0.2%	0.03%	1.9%

Density

Water at equilibrium

Compared with its other physical–chemical properties, the density of liquid water changes little. Under a pressure of 0.1 MPa, the density of air-free water is at its maximum at 3.98°C. Under these conditions, the density of water is 1000 kg m^{-3}. This is the density of

5

aqueous solutions, which is most often assumed in contaminant-transport models, even though water at 25°C under atmospheric pressure has a density of 997.02 kg m^{-3}, a relative change of 2.98% from its maximum. At the triple point of water (0.01°C), liquid water has a density of 999.78 kg m^{-3}, a relative change of –0.022% from its maximum.

Supercooled water

Speedy (1987) has presented equations that have been fitted to the thermodynamic properties of supercooled water. His equation for the density of water is

$$\rho = \rho_s \exp\left\{-T_s\left[\sum_{n=0} \frac{1}{n+1}B_\alpha^{(n)} \varepsilon^{n+1} + 2C_\alpha \varepsilon^{1/2}\right]\right\},$$ (4)

where ρ_s is a reference density and both $B_\alpha^{(n)}$ and C_α are empirical parameters, the values of which are presented in Table 1. A global fit of eq 4 to the density data of Hare and Sorensen (1987) yielded the following parameter estimates:

ρ_s	0.901 532 859 3
C_α	–0.001 176 165 2
$B_\alpha^{(0)}$	0.003 844 238 2
$B_\alpha^{(1)}$	–0.015 727 076 1
$B_\alpha^{(2)}$	0.074 406 461 4
$B_\alpha^{(3)}$	–0.140 643 265 3

The largest deviation of the fitted curve from measured data is 0.20%.

Viscosity

The viscosity of liquid water increases exponentially with decreasing temperature. While the International Association for the Properties of Water and Steam (IAPWS) has released an elaborate expression for calculating the viscosity of water as a function of pressure and temperature, a much simpler expression may be used accurately for common pressures and temperatures between –40 and 25°C. Experimental viscosity data have been fitted to the empirical Vogel–Tammann–Fulcher (VTF) equation:

$$v = v_0 \exp\left(\frac{B}{t+t_0}\right)$$ (5)

where $v_0 = 0.028\ 556$ Pa s
$B = 509.53$°C
t = temperature (°C)
t_0 = empirical constant equal to 123.15°C.

A modification of this equation is able to fit the available data more closely:

$$v = v_0 \exp\left(\frac{B_1}{t+t_0} + \frac{B_2}{(t+t_0)^2} + \frac{B_3}{(t+t_0)^3}\right).$$ (6)

where $v_0 = 0.000\ 046\ 01$ Pa s
$B_1 = 3068.6$°C
$B_2 = -3.3775 \times 10^5$ °C^2
$B_3 = 1.4781 \times 10^7$ °C^3.

This relation is plotted in Figure 3, showing its agreement with measured values.

In the temperature range of –35°C to 0°C, the viscosity of supercooled water may be fitted to Speedy's (1987) limiting-temperature empirical equation (eq 3). This relation is presented in Figure 4.
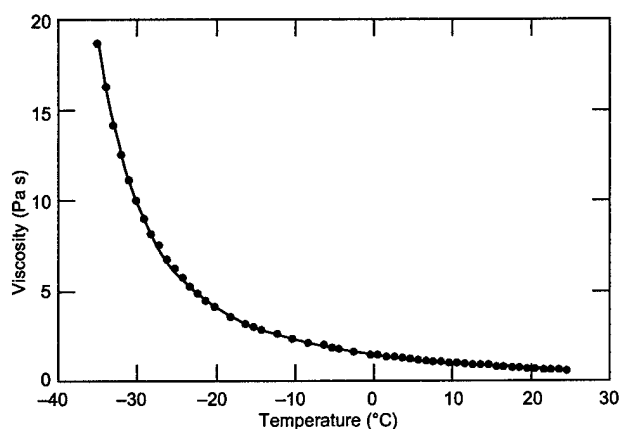
6

Figure 3. Supercooled water viscosity modeled by modified Vogel–Tammann–Fulcher (VTF) equation.
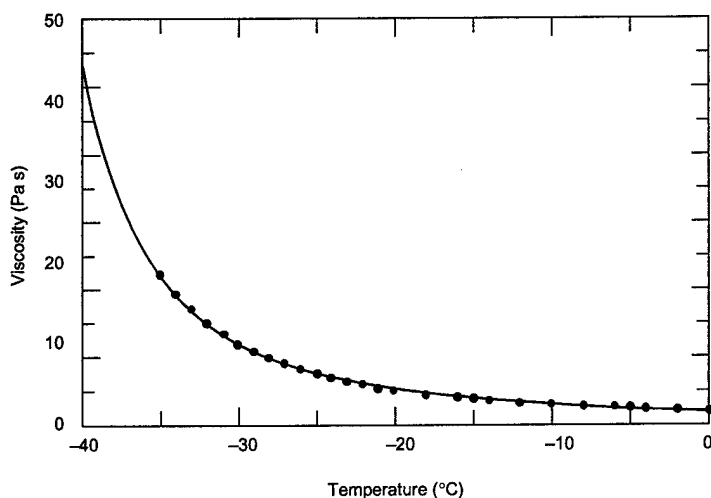
Figure 4. Supercooled water viscosity estimated by Speedy's (1987) empirical formula.

In addition to temperature, the viscosity of aqueous solutions is affected by the type and concentration of solutes. These effects are discussed in standard references (e.g., Harned and Owen 1958, Robinson and Stokes 1959). Vand (1948) derived an equation

$$\ln v_{rel} = \frac{A_3 c}{1 - Q' c} \tag{7}$$

where v_{rel} is the ratio of the solution's viscosity to that of the water.

This author found that an extension of the Vand equation gave improved fits to viscosities of NaCl solutions:

$$\ln v_{rel} = \frac{(A_0 + A_1 T)c}{1 - (Q'_0 + Q'_1 T)c}. \tag{8}$$

This equation was fitted to the data of Lyle and Hosking (1902), who reported the viscosity of NaCl solutions with initial concentrations (at 15°C) of 0.1, 0.2, 0.5, 1.0, 2.0, and 4.0 mol dm^{-3}. The following parameter estimates (and standard errors of the estimates) were obtained: $A_0 = -0.116\ 90$ (0.003 97), $A_1 = 0.000\ 579$ (0.000 012), $Q'_0 = 0.440\ 930$ (0.003 467), and $Q'_1 = -0.001\ 065\ 909\ 6$ (0.000 000 000 00).

7

Figure 5. Predicted viscosity of aqueous NaCl solutions as affected by temperature and solution concentration.

This relation and an equation that describes the viscosity of supercooled water (e.g., eq 6 or eq 3) allow one to predict the v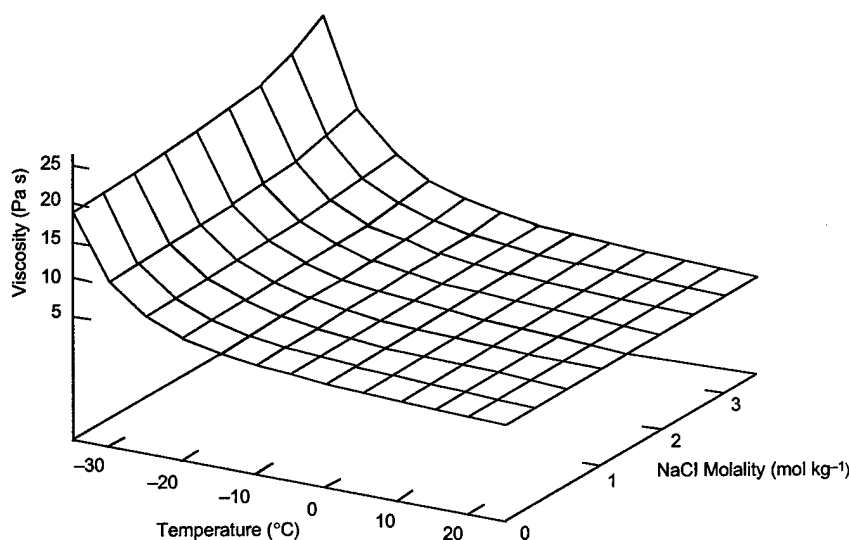iscosity of electrolyte solutions at low temperatures, though predictions at high molalites or low temperatures may be subject to significant extrapolation errors. To the author's knowledge, there are no measurements of viscosities of electrolyte solutions at subzero temperatures in the published literature. A plot of the likely interaction between temperature and electrolyte molality on the viscosity of aqueous solutions is presented in Figure 5.

Interfacial tension of liquid water against its vapor

The interfacial tension of water against air (in N m^{-1}) from the triple point of water (0.01°C) to the critical point of water (374.15°C) has been fitted to

$$\gamma_{wa} = \gamma_0 \left(\frac{T_1 - T}{T_1} \right)^u \left(1 - v \frac{T_1 - T}{T_1} \right) \tag{9}$$

in which the parameters have the following recommended values: $\gamma_0 = 0.2358$ N m^{-1}, $T_1 = 647.15$ K, $u = 1.256$, and $v = 0.625$. While there have been few reported measurements of γ_{wa} below 0°C, these data indicate that eq 9 is approximately valid to at least –8°C (Haar et al. 1984). The complexity of eq 9 belies the fact that the interfacial tension of water against its vapor is virtually linear from –10°C to 50°C, as can be seen in Figure 6.

Interfacial tension of liquid water against ice

Apparently, the most precise measurement of the interfacial tension of liquid water against ice is that of Ketcham and Hobbs (1966), who reported a value of γ_{iw} ($p = 0.101325$ MPa, $t = 0$°C) = 0.033 N m^{-1}. A compilation of other, earlier measurements was presented by Jellinek (1972).

Heat capacity

Heat capacity is the fundamental physical–chemical quantity by which changes in entropy and enthalpy with temperature can be calculated. Given the chemical and biological importance of water, it is understandable that equilibrium heat capacities of pure liquid water and ice phases have been measured precisely for most temperatures and pressures. In recent years, the heat capacities of supercooled water have been measured with ever-increasing precision.

8
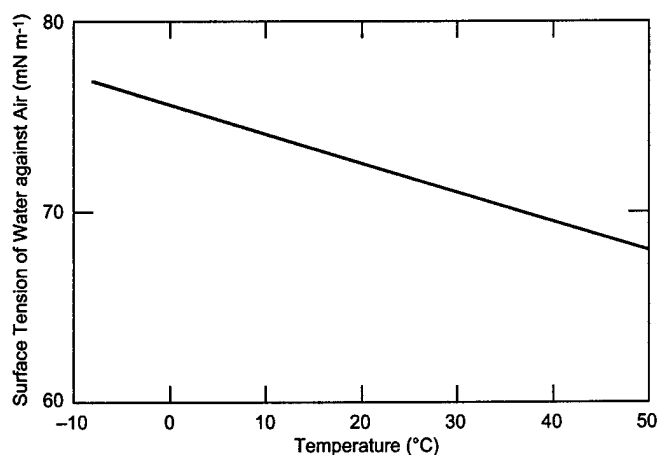
Figure 6. Measured values of interfacial tension of water against its vapor at a range of temperatures.

Water at equilibrium

The heat capacity of liquid water can be calculated accurately from the equation of state for liquid water. The equation-of-state models for water are comprehensive and algebraically complex. Fortunately, there are several computer programs available (Harr et al. 1976, Hill 1990) that can be used to calculate accurately the thermodynamic properties, including heat capacity.

Supercooled water

As noted above, Speedy (1987) has presented equations for the various thermodynamic properties of supercooled water. His expression for the constant-pressure heat capacity of supercooled water is

$$C_p = \sum_{n=0} B_{C_p}^{(n)} \varepsilon^n + 2C_{C_p} \varepsilon^{-1/2}. \tag{10}$$

The regression estimates of these parameters are presented in Table 1. Figure 7 presents the isobaric heat capacity of water as calculated by the models of Hill (1990) and Speedy (1987).

Figure 7. Heat capacity of water as predicted by Hill's (1990) equation-of-state model (for $t \le 0°C$) and Speedy's (1987) empirical formula (for $t < 0°C$).

9

Chemical properties

Thermodynamic properties

To calculate the chemical thermodynamic properties of aqueous solutions below 0°C, the relevant properties of the solvent must be calculated. The conventional reference temperature and pre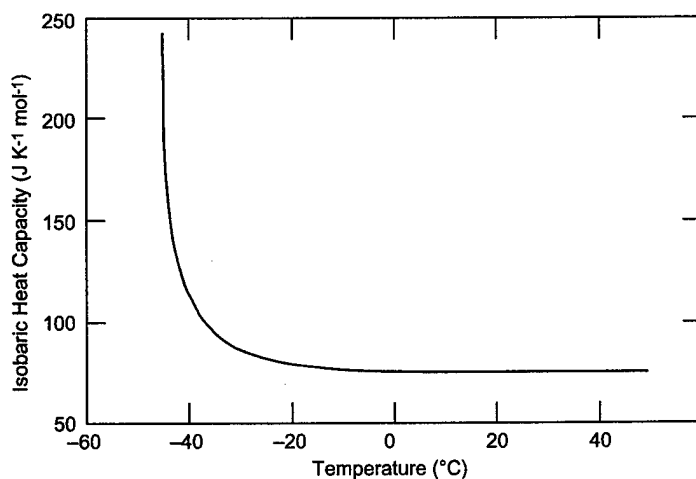ssure (298.15 K and 0.1 MPa) are inappropriate because of Speedy's (1987) empirical model upper limit of applicability of 273.15 K and were determined under a pressure of 1 atm. Initially then, the chemical potential of water at 273.15 K and 0.101325 MPa must be calculated.

Chemical potential of water at 273.15 K. To state the chemical potential of water at 0°C, one needs to calculate:

$$\mu^*_{H_2O(l)}\left(T_{rw}, p_{rw}\right) - \mu^*_{H_2O(l)}\left(T_{rc}, p_{rc}\right) \tag{11}$$

where T_{rc} = 298.15 K
T_{rw} = 273.15 K
T_s = 227.15 K
p_{rc} = 0.1
p_{rw} = 0.101325 MPa.

Equation 11 can be evaluated with

$$\mu^*_B\left(T_{rw}, p_{rw}\right) - \mu^*_B\left(T_{rc}, p_{rc}\right)$$

$$= -\bar{S}^*_B\left(T_{rc}, p_{rc}\right)\left(T_{rw} - T_{rc}\right) + \int_{T_{rc}}^{T_{rw}} C^*_{p,B}dT \tag{12}$$

$$-T_{rw}\int_{T_{rc}}^{T_{rw}} \frac{C^*_{p,B}}{T}dT + \int_{p_{rc}}^{p_{rw}} \bar{V}^*_B\left(T_{rw}, p\right)dp$$

where μ^*_B is the chemical potential of pure B (J mol^{-1}), $\bar{S}^*_B$ is the molar entropy of pure B (J K^{-1} mol^{-1}), and $\bar{V}^*_B$ is the molar volume of pure B (m^3 mol^{-1}).

Equation 12 is equivalent to

$$\mu^*_B\left(T_{rw}, p_{rw}\right) - \mu^*_B\left(T_{rc}, p_{rc}\right) = -\bar{S}^*_B\left(T_{rc}, p_{rc}\right)\left(T_{rw} - T_{rc}\right) + \left[\bar{H}^*_B\left(T_{rw}, p_{rc}\right) - \bar{H}^*_B\left(T_{rc}, p_{rc}\right)\right]$$

$$-T_{rw}\left[\bar{S}^*_B\left(T_{rw}, p_{rc}\right) - S^*_B\left(T_{rc}, p_{rc}\right)\right] + \int_{p_{rc}}^{p_{rw}} \bar{V}^*_B\left(T_{rw}, p\right)dp \tag{13}$$

where $\bar{H}^*_B$ is the molar enthalpy of pure B (J mol^{-1}).

Standard reference tables (e.g., Chase et al. 1985) provide some of the required values:

$$\bar{S}^*_{H_2O(l)}\left(T_{rc}, p_{rc}\right) = 69.950 \, J \, K^{-1} \, mol^{-1}.$$

The equation-of-state model for water (Hill 1990) can be used to calculate some of the terms directly:

$$S_{H_2O(l)}\left(T_{rw}, p_{rc}\right) - S^*_{H_2O(l)}\left(T_{rc}, p_{rc}\right) = -6.616\,04 \, J \, K^{-1} mol^{-1}$$

$$H_{H_2O(l)}\left(T_{rw}, p_{rc}\right) - H^*_{H_2O(l)}\left(T_{rc}, p_{rc}\right) = -1.88\,547 \, kJ \, mol^{-1}$$

$$\bar{V}^*_{H_2O(l)}\left(T_{rw}, p_{rc}\right) = 0.018\,018\,09 \, dm^3 \, mol^{-1}$$

10

The most recent accurate measurement of the enthalpy of fusion for water to ice appears to be that of Haida et al. (1974), who reported

$$\Delta_s^l \overline{H}_{H_2O}^* \left(T_{rw}, p_{rc}\right) = 6006.8 \ \text{J} \ \text{mol}^{-1}.$$

By the relation (McGlashan 1979)

$$\Delta_\beta^\alpha \overline{H}_B^* = T_{\alpha+\beta} \, \Delta_\beta^\alpha S_B^* \tag{14}$$

we find that

$$\Delta_s^l \overline{S}_{H_2O}^* \left(T_{rw}, p_{rc}\right) = 21.990\,85 \ \text{J} \ \text{K}^{-1} \text{mol}^{-1} \tag{15}$$

which allows the evaluation of eq 12:

$$\mu_B^* \left(T_{rw}, p_{rw}\right) - \mu_B^* \left(T_{rc}, p_{rc}\right) = -\overline{S}_B^* \left(T_{rc}, p_{rc}\right)\left(T_{rw} - T_{rc}\right)\overline{H}_B^* \left(T_{rw}, p_{rc}\right) - \overline{H}_B^* \left(T_{rc}, p_{rc}\right) \tag{16}$$

$$-T_{rw}\left[\overline{S}_B^* \left(T_{rw}, p_{rc}\right) - \overline{S}_B^* \left(T_{rc}, p_{rc}\right)\right] + \int_{p_{rc}}^{p_{rw}} \overline{V}_B^* \left(T_{rw}, p\right) dp + \int_{p_{rc}}^{p_{rw}} \overline{V}_B^* \left(T_{rw}, p\right) dp = 1.667\ 37 \ \text{kJ} \ \text{mol}^{-1}$$

Supercooled water

The standard-state chemical potential of supercooled water at temperatures between 0°C and –46°C under pressures of 1 atm can also be calculated by eq 12. In this temperature range, the changes in $C_{p,H_2O(l)}^*$ are described by eq 10. The definite integrals needed to make these calculations are as follows:

$$\int_{T_{rw}}^{T_f} \frac{C_{p,H_2O(l)}^*}{T} dT = \frac{B_{C_p}^{(4)}\left(T_f^4 - T_{rw}^4\right)}{4T_s^4} + \frac{\left[B_{C_p}^{(3)} - 4B_{C_p}^{(4)}\right]\left(T_f^3 - T_{rw}^3\right)}{3T_s^3} + \frac{\left[B_{C_p}^{(2)} - 3B_{C_p}^{(3)} + 6B_{C_p}^{(4)}\right]\left(T_f^2 - T_{rw}^2\right)}{2T_s^2}$$

$$+ \frac{\left[B_{C_p}^{(1)} - 2B_{C_p}^{(2)} + 3B_{C_p}^{(3)} - 4B_{C_p}^{(4)}\right]\left(T_f - T_{rw}\right)}{T_s} + 2C_{C_p} \arctan\left(\sqrt{\frac{T_f}{T_s} - 1}\right)$$

$$- 2C_{C_p} \arctan\left(\sqrt{\frac{T_{rw}}{T_s} - 1}\right) + \left[B_{C_p}^{(0)} - B_{C_p}^{(1)} + B_{C_p}^{(2)} - B_{C_p}^{(3)} + B_{C_p}^{(4)}\right] \times \left[\ln(T_f) - \ln(T_{rw})\right] \tag{17}$$

and

$$\int_{T_{rw}}^{T_f} C_{p,H_2O(l)}^* \, dT = \left(B_{C_p}^{(0)} - B_{C_p}^{(1)} + B_{C_p}^{(2)} - B_{C_p}^{(3)} + B_{C_p}^{(4)}\right)\left(T_f - T_{rw}\right) + \frac{B_{C_p}^{(4)}\left(T_f^5 - T_{rw}^5\right)}{5T_s^4}$$

$$+ \frac{\left[B_{C_p}^{(3)} - 4B_{C_p}^{(4)}\right]\left(T_f^4 - T_{rw}^4\right)}{4T_s^3} + \frac{\left[B_{C_p}^{(2)} - 3B_{C_p}^{(3)} + 6B_{C_p}^{(4)}\right]\left(T_f^3 - T_{rw}^3\right)}{3T_s^2}$$

$$+ \frac{\left[B_{C_p}^{(1)} - 2B_{C_p}^{(2)} + 3B_{C_p}^{(3)} - 4B_{C_p}^{(4)}\right]\left(T_f^2 - T_{rw}^2\right)}{2T_s} + 2C_{C_p} \, T_s\left(\sqrt{\frac{T_f}{T_s} - 1} - \sqrt{\frac{T_{rw}}{T_s} - 1}\right). \tag{18}$$

11

Chemical thermodynamics of mixtures and aqueous solutions

Before considering the properties of electrolyte solutions at subzero temperatures, this discussion surveys briefly the chemical thermodynamics of mixtures and solutions. Consider a mixture of N components:

$$n_T = n_A + n_B + \ldots + n_N \tag{19}$$

where n_A, n_B ... are the amounts of components A, B ... (mol) and n_T total number of molecules in the mixture (mol). If the number of molecules of one component is much greater than all the other components, the mixture is called a solution. The dominant mixture component is called the solvent, and the other mixture components are called solutes. If the mixture being discussed is a solution, by convention the letter A is reserved to represent the solvent.

Consider now a binary mixture or solution:

$$n_T = n_A + n_B. \tag{20}$$

For all extensive thermodynamic properties of the mixture or solution, the partial molar quantities can be defined; for example, the partial molar volume of B ($m^3\ mol^{-1}$) is

$$\overline{V}_B \overset{\text{def}}{=} \left(\frac{\partial V_T}{\partial n_B} \right)_{p,T,n_i \ni i \neq B} \tag{21}$$

where V_T is the total volume of the mixture (m^3) and $\ni$ is a logical symbol for "such that." The total volume of the binary mixture is therefore

$$V_T = n_A \overline{V}_A + n_B \overline{V}_B. \tag{22}$$

We can perform a similar operation on the total Gibbs energy[1] (G_T, J) of the mixture,

$$G_T = n_A \overline{G}_A + n_B \overline{G}_B \tag{24}$$

where the partial molar Gibbs energy,

$$\overline{G}_B \overset{\text{def}}{=} \left(\frac{\partial G_T}{\partial n_B} \right)_{p,T,n_i \ni i \neq B} \tag{25}$$

is defined similarly to before. And, as before, the total Gibbs energy can be represented in terms of partial molar quantities:

$$G_T = n_A \overline{G}_A + n_B \overline{G}_B. \tag{26}$$

The partial molar Gibbs energy is also known as the chemical potential

$$\mu_B \overset{\text{def}}{=} \overline{G}_B. \tag{27}$$

In a mixture, the chemical potential of each component differs from some defined standard state. This difference defines the activity of the mixture component,

---

[1] This quantity is defined by:

$$G_T \overset{\text{def}}{=} H_T - TS_T \tag{23}$$

where H_T is total enthalpy (J) and S_T is total entropy ($J\ K^{-1}$).

12

$$\mu_B = \mu_B^{\ominus} + RT \ln a_B,$$ (28)

where $\mu_B^{\ominus}$ is the standard-state chemical potential of component B and a_B is its activity. In many cases, the activity of a mixture component can be approximated by its mole fraction, defined by

$$x_B = \frac{n_B}{n_T},$$ (29)

or its molality, defined by

$$m_B = \frac{n_B}{(n_A M_A)}$$ (30)

where M_A is the molar mass of solvent A (kg mol^{-1}).

These approximations are imperfect, so the deviation of the mole fraction or molality from the activity defines an activity coefficient (f_B or γ_B), termed rational if the reference function is the mole fraction:

$$\mu_B = \mu_B^{\ominus} + RT \ln(f_B x_B),$$ (31)

or molality-based if the reference function is solution molality:

$$\mu_B = \mu_B^{\ominus} + RT \ln\left(\frac{\gamma_B m_B}{m_B^{\ominus}}\right)$$ (32)

where $m_B^{\ominus}$ is the standard state molality, 1 mol kg^{-1}.

Electrolyte solutions

Geochemical solutions are electrolyte solutions. Because electrolytes dissolve into charged ions in solution, the chemical–thermodynamic description of these solutions is much more difficult than for solutions and mixtures of electrically neutral components.

Consider the simple case of an unhydrated crystalline $B_{\nu_B} C_{\nu_C}$ (cr) composed of ν_C moles of anion C^{z_C} and B^{z_B} (z_B and z_C are the charge numbers of the subscripted ions) that dissolves completely in water to form an anionic and a cationic species:

$$B_{\nu_B} C_{\nu_C} \text{ (cr)} = \nu_B B^{z_B} \text{(aq)} + \nu_C C^{z_C} \text{(aq)}.$$ (33)

The single-ion activity coefficient γ_B can be defined by

$$a_{B(aq)} \stackrel{\text{def}}{=} \frac{\gamma_B m_B}{m_B^{\ominus}}$$ (34)

and related to the chemical potential of the single-ion species by

$$\mu_{B(aq)} = \mu_{B(aq)}^{\ominus} + RT \ln\left(\frac{m_B \gamma_B}{m_B^{\ominus}}\right).$$ (35)

For m_{BC} moles of salt, which dissociate into $\nu_B m_{BC}$ moles of cation and $\nu_C m_{BC}$ moles of anion, the chemical potentials for the salt μ_{BC} in solution is related to the chemical potentials for the single-ion species by

$$m_{BC} \mu_{BC(aq)} = m_B \mu_{B(aq)} + m_C \mu_{C(aq)}$$ (36)

(From eq 37, the salt $B_{\nu_B} C_{\nu_C}$ will be represented simply as BC). The chemical potentials of the electrolyte and the single-ion species are related by

$$\mu_{BC} = \nu_B \mu_B + \nu_C \mu_C$$ (37)

13

which leads to

$$\mu_{BC} = \nu_B\,\mu_B^\Theta + \nu_C\,\mu_C^\Theta + \nu_B RT\ln(m_B\gamma_B) + \nu_C RT\ln(m_C\gamma_C) \tag{38}$$

and

$$\mu_{BC} = \mu_{BC}^\Theta + (\nu_B + \nu_C)RT\ln\left[m_{BC}\left(\nu_C^{\nu_B}\,\nu_B^{\nu_C}\right)^{1/(\nu_B+\nu_C)}\gamma_{\pm BC}\right]. \tag{39}$$

By

$$\mu_{BC}^\Theta = \nu_C\,\mu_C^\Theta + \nu_B\,\mu_B^\Theta \tag{40}$$

the mean-ionic activity coefficient is therefore defined as

$$\gamma_{\pm BC} \overset{\text{def}}{=} \left(\gamma_B^{\nu_B}\gamma_C^{\nu_C}\right)^{\frac{1}{(\nu_B+\nu_C)}}. \tag{41}$$
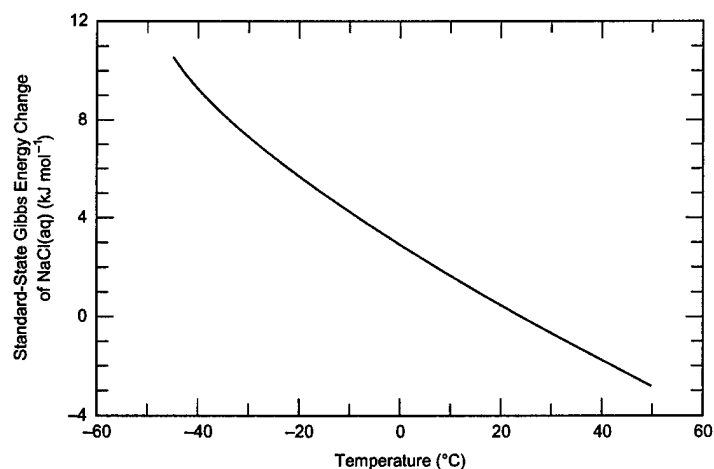

Figure 8. Standard-state chemical potential of NaCl(aq) as function of temperature.
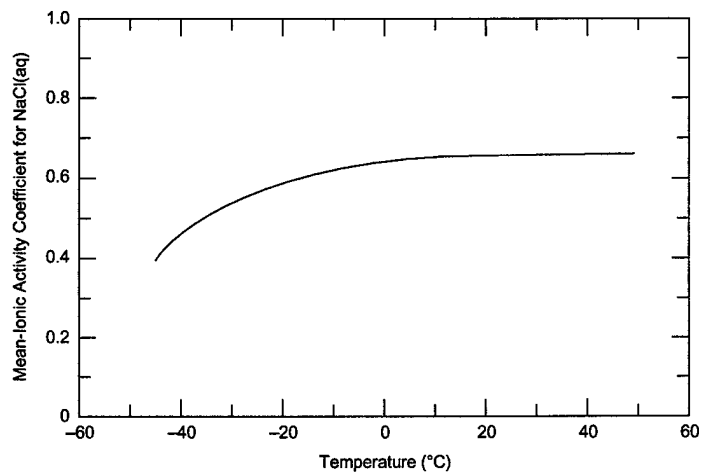

Figure 9. Mean-ionic activity coefficient of NaCl(aq) (p = 0.1 MPa, m = 1.0 mol kg^{-1}) as function of temperature.

14

Chemical equilibrium modeling considerations

To model the chemistry of any aqueous electrolyte solution, the chemical potential of each modeled constituent must be estimated either explicitly or implicitly. The most efficient means of estimating the single-ion chemical potential of a solute is by

$$\mu_{B(aq)} = \mu_{B(aq)}^{\ominus} + RT\ln\left(\frac{m_B \gamma_B}{m_B^{\ominus}}\right). \tag{35}$$

Both the standard-state chemical potential of the solute [$\mu_{B(aq)}^{\ominus}$] and the single-ion activity coefficient γ_B are affected by temperature. These effects are presented in Figures 8 and 9. Further, ice is nearly a pure phase. As aqueous solutions are cooled below their freezing points, ice forms, excluding solutes to the remaining liquid-water solutions. Accordingly, the aqueous solutions at subzero temperatures are typically brines, the activity coefficients for which must be estimated by elaborate models such as that of Pitzer and his coworkers. (For a further discussion, see Pitzer 1991 and Spencer et al. 1990.) Figure 10 shows the isothermal, isobaric changes in the activity coefficient of a salt (NaCl) with its concentration.

Colligative properties: freezing point depression
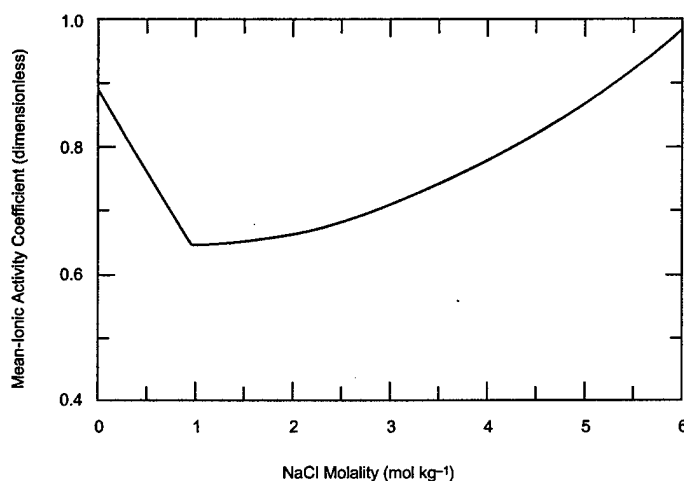
Figure 10. Mean-ionic activity coefficient of NaCl(aq) (p = 0.1 MPa, T = 298.15 K) as function of molality.

While liquid water is an almost universal solvent, ice is generally a very pure phase. The freezing point of an aqueous solution is depressed proportionately to the concentrations of its solutes. The thermodynamics of this behavior is fairly straightforward. The discussion here follows closely that of Atkins (1990).

At equilibrium, the chemical potentials of the solvent in the liquid and solids phases are equal:

$$\mu_A(s) = \mu_A(l). \tag{36}$$

Since the standard state for the solvent is pure solvent substance:

$$\mu_A^{\ominus}(l) \overset{\text{def}}{=} \mu_A^*(l) \tag{37}$$

by eq 29 the following relation can be derived:

$$\mu_A^*(s) = \mu_A^*(l) + RT^{s+l}\ln a_A \tag{38}$$

is obtained, T^{s+l} representing the freezing temperature. If it is assumed that $a_A \equiv x_A$ (i.e., $f_A \equiv 1$),

15

$$\mu_A^*(s) = \mu_A^*(l) + RT^{s+l} \ln x_A. \tag{39}$$

As with total thermodynamic properties (eq 25), the Gibbs energies, enthalpies, and entropies of fusion are related by

$$\Delta_s^l \overline{G}_{H_2O}^*(T,p) = \Delta_s^l \overline{H}_{H_2O}^*(T,p) - T\Delta_s^l \overline{S}_{H_2O}^*(T,p). \tag{40}$$

From this expression, we can obtain directly

$$\ln x_A \frac{\mu_A^*(s) - \mu_A^*(l)}{RT^{s+l}} = \frac{\Delta_s^l \overline{H}_{H_2O}^*(T,p)}{RT^{s+l}} - \frac{\Delta_s^l \overline{S}_{H_2O}^*(T,p)}{R}. \tag{41}$$

Recalling that for a binary solution

$$x_A + x_B = 1$$

one can calculate the molar Gibbs energy of fusion for two systems: a pure solvent and a solution.

For the pure solvent system,

$$\ln 1 = 0 = \frac{\mu_A^*(s) - \mu_A^*(l)}{RT^{s+l,*}} = \frac{\Delta_s^l \overline{H}_{H_2O}^*(T^*,p)}{RT^{s+l,*}} - \frac{\Delta_s^l \overline{S}_{H_2O}^*(T^*,p)}{R} \tag{42}$$

and for the solution system,

$$\ln(1 - x_B) = \frac{\mu_A^*(s) - \mu_A^*(l)}{RT^{s+l}} = \frac{\Delta_s^l \overline{H}_{H_2O}^*(T,p)}{RT^{s+l}} - \frac{\Delta_s^l \overline{S}_{H_2O}^*(T^*,p)}{R} \tag{43}$$

where $T^{s+l,*}$ is the freezing point of the pure solvent system. Subtracting one from the other, we obtain

$$\ln(1 - x_B) = \frac{\Delta_s^l \overline{H}_{H_2O}^*(T,p)}{RT^{s+l}} - \frac{\Delta_s^l \overline{H}_{H_2O}^*(T^*,p)}{RT^{s+l,*}}. \tag{44}$$

With small error, it can be assumed that the enthalpy of fusion changes insignificantly with small changes in temperature, that is,

$$\Delta_s^l \overline{H}_{H_2O}^*(T,p) \approx \Delta_s^l \overline{H}_{H_2O}^*(T^*,p). \tag{45}$$

This leads immediately to

$$\ln(1 - x_B) = \frac{\Delta_s^l \overline{H}_{H_2O}^*(T,p)}{R} \left(\frac{1}{T^{s+l}} - \frac{1}{T^{s+l,*}} \right) \tag{46}$$

If it is further assumed that $\ln(1 - x_B) \approx -x_B$ and that $T^{s+l} \approx T^{s+l,*}$.

An approximate expression for the freezing-point depression is therefore provided:

$$\Delta T = \left(\frac{RT^{*2}}{\Delta_s^l \overline{H}_{H_2O}^*(T,p)} \right) x_B \tag{47}$$

where $\Delta T = T^{s+l,*} - T^{s+l}$.

Equation 47 suggests that freezing-point depression is a solvent property. This observation has been formalized in the definition of a cryoscopic constant, K_f, for a given solvent:

$$\Delta T = K_f \, m_B \tag{48}$$

which for water is 1.86 K kg mol^{-1}.

The freezing point is actually a phase-equilibrium line along which, as the temperature of a system decreases, a largely pure ice phase is in equilibrium with increasingly concentrated aqueous solutions. Examples of this behavior can be seen in Figures 11 and 12, which
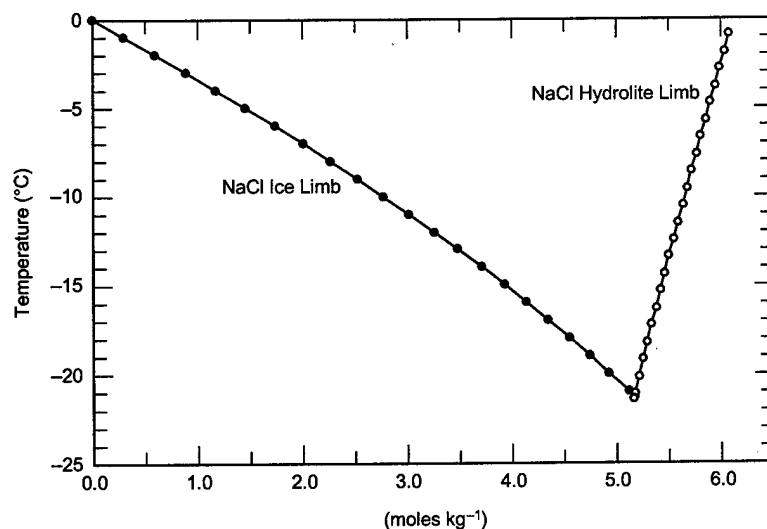

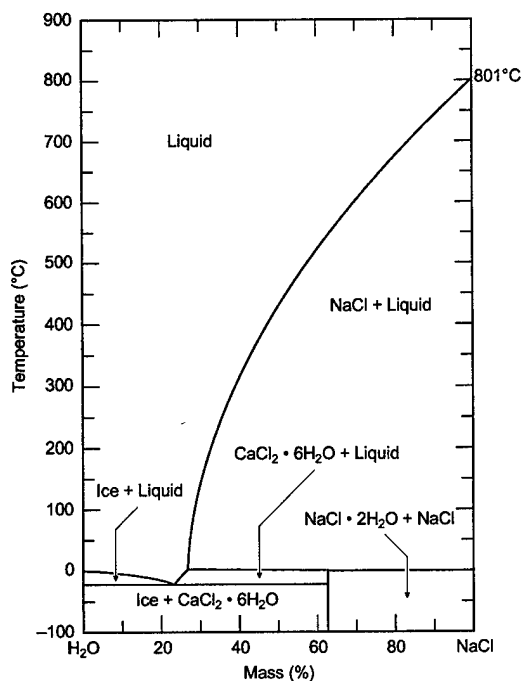Figure 11. Phase diagram for NaCl-H$_2$O system. (Courtesy of Dr. G.M. Marion, USACRREL.)

Figure 12. Phase diagram for CaCl$_2$-H$_2$O system. (Courtesy of Dr. G.M. Marion, USACRREL.)

17

present phase diagrams of the NaCl–H$_2$O and CaCl$_2$–H$_2$O systems under atmospheric pressure. It is helpful to recall the phase rule when examining these phase diagrams. For nonreacting systems, the phase rule states

$$F = C + 2 - P \tag{55}$$

where F is the degrees of freedom, C is the number of components, and P is the number of phases (McGlashan 1979). A two-phase system (i.e., ice–NaCl solution) that is composed of two components (i.e., NaCl and H$_2$O) has (2 + 2 − 2) two degrees of freedom, that is, fixing two independent variables will specify the state of the system. Three independent variables are most natural: pressure, temperature, and composition. Since pressure is fixed by the atmosphere, the choice of temperature or composition will specify the other independent variable. This dependence is represented by the ice–solution coexistence lines in Figures 11 and 12. Simple NaCl solutions with molalities above 5.2 that are cooled below 0°C will not coexist with ice but rather with a solid phase composed of hydrohalite [NaCl • 2H$_2$(cr)]. The ice–solution hydrohalite–solution coexistence curves converge at the eutectic point, the unique temperature-composition combination where these three phases coexist, a triple point that is specified entirely by the number of phases and the lone independent variable, pressure.

The phase rule can be extended to the interpretations of the freezing behavior of natural waters. When natural waters are frozen, solute effects must be considered. In particular, several salts precipitate from freezing solutions as the remaining liquid water

Figure 13. Phase diagram for seawater. (Courtesy of Dr. G.M. Marion, USACRREL.)

solutions concentrate. This progression has been studied most closely in the freezing behavior of seawater, the properties of which may be used as an approximate model for soil solutions in freezing and frozen ground. A phase diagram for seawater is presented in Figure 13.

PHYSICAL–CHEMICAL PROPERTIES OF ICE

Heat capacity

As for many solids, the heat capacity of ice as a function of temperature can be fitted to the equation of Maier and Kelly (1932):

$$C^*_{p,\text{H}_2\text{O(cr,I)}} = a + bT + \frac{c}{T^2} \tag{50}$$

where $a = -10.6644$ (1.5999) J K^{-1} mol^{-1}
$b = 0.1698$ (0.0046) J K^{-2} mol^{-1}
$c = 198\,148$ (28 230) J K mol^{-1}.

The changes in molar enthalpy and entropy can thereby be calculated via the following integrals:

$$\int_{T_\text{rw}}^{T_\text{f}} C^*_{p,\text{H}_2\text{O(cr,I)}} dT = a\left(T_\text{f} - T_\text{rw}\right) + \frac{b}{2}\left(T_\text{f}^2 - T_\text{rw}^2\right) + c\left(\frac{1}{T_\text{rw}} - \frac{1}{T_\text{f}}\right) \tag{51}$$

18
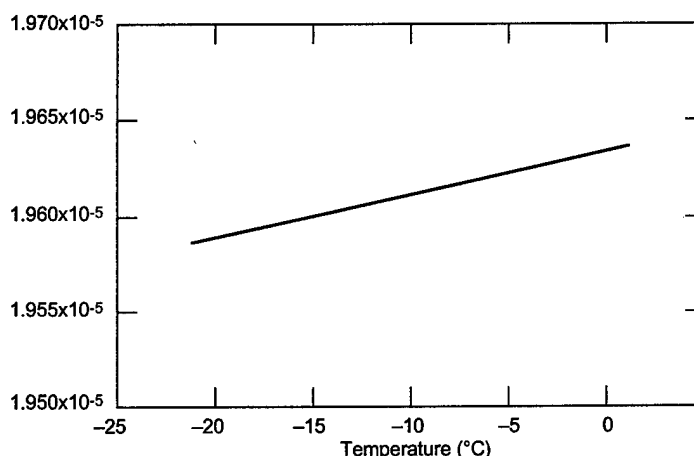
Figure 14. Molar volume of hexagonal ice under 1 atm pressure at temperatures near its melting point.

and

$$\int_{T_{rw}}^{T_f} \frac{C^*_{p,H_2O(cr,I)}}{T} \, dT = a[\ln(T_f) - \ln(T_{rw})] + b(T_f - T_{rw}) - \frac{c}{2}\left[\frac{1}{T_f^2} - \frac{1}{T_{rw}^2}\right]. \tag{52}$$

Molar volume

Water is one of the few substances for which one of its solid phases is less dense than its liquid. The molar volumes of hexagonal ice, the phase most commonly encountered in nature, at temperatures near its melting point are presented in Figure 14.

PHYSICS OF FROZEN POROUS MEDIA

Moderately cool temperatures affect the physical–chemical state of water and its propensity to flow through porous media. For contaminant transport, changing temperatures affect the chemical potentials of the solvents and solutes in the pore solutions and therefore the solubility and reactivity of the solutes. These changes in the physical properties of the solvent and chemical properties of the solutes can affect dramatically the mobility of contaminants in cold regions.

At cold temperatures, at which surficial, vadose, and aquifer waters freeze, the nature of flow changes dramatically. First, at a macroscopic level, because the effective volume of voids is reduced, ground has a much lower permeability when frozen. This affects the basin-scale hydrology in cold regions in sometimes unpredictable ways.

Second, while frozen ground is less permeable, it is not impermeable. The mathematical description of transport of solutes through frozen ground is inherently more complex than unfrozen ground for the following reasons:

1. The solvent, water, is partitioned into two phases, liquid water and ice, that are intimately commingled in the pores of the ground.

2. As the ice forms, the solutes (including the contaminants) are largely excluded from the ice, concentrating the remaining liquid-water solutions in a thin film at the colloid surfaces. The chemical potentials of the solutes in these solutions, used to estimate the effects of solute–solute and solute–surface interactions are not understood well enough to be modeled accurately.

3. In unfrozen coarse-grained soils, the movement of solutes is controlled by the Darcian flow of water in response to gravitational and pressure gradients. In frozen ground, solutes may also move appreciably in response to thermal and osmotic gradients—transport mechanisms that are less well understood and more difficult to parameterize than flow in response to gravitational and pressure gradients.

19

Darcy's law

Water flow in porous media may be described by Darcy's law, eq 1. Cold temperatures reduce water flows through porous media. As has been discussed, cold temperatures increase the viscosity of water. Freezing reduces dramatically the permeability of soils and ground. Geochemical solutions do not freeze uniformly at 0°C. The equilibrium freezing temperature of pore water is a function of pore geometry, freezing-point depressing effects of solutes, and the charge behavior of the porous matrix (Everett 1961). The quantitative description of these effects, which is discussed below, is an active research area.

Soil-water retention curve

The permeability of frozen porous media is affected by its liquid water content. Accordingly, a discussion of the physics of unsaturated porous media is appropriate.

Matric potential

Two factors have been identified in determining the relationship between matric potential and water content in unsaturated soils. The first is the pressure difference between the soil atmosphere and the liquid water bound to soil particles. The second factor is the work required to expand the liquid water/air interface as soil-water content decreases. When a stable interface is established, these two factors are balanced and the water content is stable. For a given matric potential, any environmental change that changes one of these balanced factors relative to the other can be expected to cause the water content to change.

Effect of temperature

An obvious, and pertinent, example is temperature, which decreases the interfacial tension of water against air. The effect of temperature on the soil-water retention curve may be estimated via

$$\left(\frac{\partial \theta}{\partial T}\right)_{\Psi} = -\left(\frac{\partial \theta}{\partial \Psi}\right)_t \left(\frac{\partial \Psi}{\partial T}\right)_{\theta} \tag{53}$$

where θ is the volumetric water content of the porous medium (dimensionless), and Ψ is the matric potential of the water in the porous medium (Pa).

For a given pore radius, the relationship between capillary pressure and interfacial tension is direct:

$$\Psi = -\frac{(2\gamma_{wa}\cos\phi)}{r} \tag{54}$$

where r is pore radius (m) and ϕ is the contact angle of the air/water interface with the solid (rad). The partial derivative in the denominator of eq 54 can be calculated with the formula recommended by eq 9:

$$\frac{\partial \gamma_{wa}}{\partial T} = \gamma_0 \, T_1^{-2}\left(1 - \frac{T}{T_1}\right)^{u-1} [(uv + v)(T - T_1) - uT_1]. \tag{55}$$

Accordingly, one would expect that the following relationship would hold exactly:

$$\frac{\left[\dfrac{\partial \Psi(t,\theta)}{\partial T}\right]}{\left[\dfrac{\partial \gamma_{wa}(t)}{\partial T}\right]} = \frac{\Psi(t,\theta)}{\gamma_{wa}(t)} \; . \tag{56}$$

In fact it does not, requiring the definition of an empirical variable [$G(\theta)$] introduced by Nimmo and Miller (1986) to account for the discrepancy:

20

$$G(\theta) = \frac{\dfrac{\Psi(t_2,\theta)}{\Psi(t_1,\theta)} - 1}{\dfrac{\gamma_{wa}(t_2)}{\gamma_{wa}(t_1)} - 1} \quad \text{(where } t_2 > t_1\text{)}.$$

(57)

Soil freezing characteristic curve

Liquid water (albeit generally very small amounts) exists in frozen soil at temperatures significantly below 0°C. For water-saturated frozen soils, an approximation of the liquid-water content can be calculated from the soil-water retention curve, if known. The physics of the two situations are similar: in unsaturated, unfrozen soil, the liquid-water content is determined by the balancing of the pressure difference across the interface between the soil water and the soil atmosphere with the work necessary to deform this interface against the interfacial tension of water against air. The validity of this hypothetical mechanism for controlling the soil-water retention curve is supported by the observation that, for a given matric potential, the quantity of water held by the soil decreases as the temperature increases; that is, as interfacial tension decreases with increasing temperatures, less work is required to deform the air/water interface.

In frozen, water-saturated soils, there is a water/ice interface between the liquid water surrounding the soil particles and the ice. This situation is qualitatively similar to the water/air interface that exists in unsaturated soils. A schematic displaying these parallel physical systems is presented in Figure 15. It is expected then that, for a single soil sample of unaltered internal structure, liquid water contents in the frozen, unsaturated state should be a function of the pressure gradient across the water/ice interface. This function should be similar to the empirical equation that describes the soil-water retention curve.
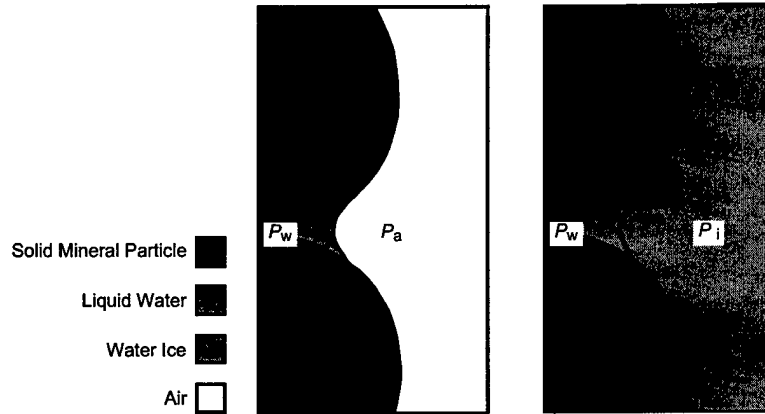
Figure 15. The similarity of capillary water of unsaturated, unfrozen soils and unfrozen water in saturated, frozen soils.

Generalized Clapeyron equation

Here we follow closely the lucid, complete presentation of the chemical–thermodynamic theory of frozen porous media presented by Brun et al. (1977). Consider three phases: solid (s), liquid (l), and gas (g), which are in thermal, but not necessarily in hydrostatic, equilibrium (i.e., $T_s = T_l = T_g = T$, but $p_s \neq p_l \neq p_g$). Their development begins with two sets of classic equalities: the Gibbs–Duhem equations, and the Kelvin equation.

Gibbs–Duhem equations. For each phase, the Gibbs–Duhem relation holds:

$$0 = S_m^g \, dT - V_m^g \, dp^g + \sum_B x_B^g d\mu_B^g$$

$$0 = S_m^l \, dT - V_m^l \, dp^l + \sum_B x_B^l d\mu_B^l$$

(58)

$$0 = S_m^s \, dT - V_m^s \, dp^s + \sum_B x_B^s d\mu_B^s$$

21

where S_m^g, S_m^l, and S_m^s are the molar entropies (J K^{-1} mol^{-1}) of the gas, liquid, and solid phases, respectively; V_m^g, V_m^l, and V_m^s are their molar volumes (m^3 mol^{-1}); x_B^g, x_B^l, and x_B^s are the mole fractions of component B in the three phases; and μ_B^g, μ_B^l, and μ_B^s are the chemical potentials (J mol^{-1}) of component B in the three phases.

Kelvin equations. The Kelvin equations give the pressure gradients across the gas/solid and liquid/solid interfaces in terms of the differential geometry of these interfaces:

$$p^g - p^s = \gamma^{sg} \frac{dA_{s,m}^{sg}}{dV_m^g} \tag{59}$$

$$p^l - p^s = \gamma^{ls} \frac{dA_{s,m}^{ls}}{dV_m^l} \tag{60}$$

where $A_{s,m}^{ls}$ and $A_{s,m}^{sg}$ (m^2 mol^{-1}) are the molar areas of the liquid/solid and solid/gas interfaces, respectively, and γ^{ls} and γ^{sg} (N m^{-1}) are the corresponding interfacial tensions. Capillary pressures of liquid phases can be estimated by applying these equalities.

If the solid, liquid, and vapor phases are pure, then eq 67 can be rewritten:

$$0 = S_{m,H_2O}^{*g} dT - V_{m,H_2O}^{*g} dp^g + d\mu_{H_2O}^{*g} \tag{61}$$

$$0 = S_{m,H_2O}^{*l} dT - V_{m,H_2O}^{*l} dp^l + d\mu_{H_2O}^{*l} \tag{62}$$

$$0 = S_{m,H_2O}^{*s} dT - V_{m,H_2O}^{*s} dp^s + d\mu_{H_2O}^{*s} \tag{63}$$

where the superscript * indicates a pure phase. By taking the partial derivatives of eqs 68 and 69, dp^g and dp^l can be related to dp^s by

$$dp^g = dp^s + d\left(\gamma^{sg} \frac{dA_{s,m}^{sg}}{dV_m^g} \right) \tag{64}$$

and

$$dp^l = dp^s + d\left(\gamma^{ls} \frac{dA_{s,m}^{ls}}{dV_m^l} \right). \tag{65}$$

By subtracting eq 67 from eq 69, and 69 from 68, then subtracting the latter difference from the former, the following relation is obtained after rearrangement:

$$\left(\frac{S_{m,H_2O}^{*s} - S_{m,H_2O}^{*g}}{V_{m,H_2O}^{*s} - V_{m,H_2O}^{*g}} - \frac{S_{m,H_2O}^{*l} - S_{m,H_2O}^{*s}}{V_{m,H_2O}^{*l} - V_{m,H_2O}^{*s}} \right) dT =$$

$$\frac{V_{m,H_2O}^{*g}}{V_{m,H_2O}^{*g} - V_{m,H_2O}^{*s}} d\left(\gamma^{sg} \frac{dA_{s,m}^{sg}}{dV_m^g} \right) - \frac{V_{m,H_2O}^{*l}}{V_{m,H_2O}^{*l} - V_{m,H_2O}^{*s}} d\left(\gamma^{ls} \frac{dA_{s,m}^{ls}}{dV_m^l} \right). \tag{66}$$

By noting that $V_{m,H_2O}^{*g} \gg V_{m,H_2O}^{*l}$ and by assuming that

$$\gamma^{sg} \frac{dA_{s,m}^{sg}}{dV_m^g} = 0,$$

the following relation is obtained:

$$\left(S^{*l}_{m,H_2O} - S^{*s}_{m,H_2O}\right)dT = V^{*l}_{m,H_2O}\,d\left(\gamma^{ls}\frac{dA^{ls}_{s,m}}{dV^{l}_m}\right).$$ (67)

By defining liquid–solid capillary pressure (Pa), p^{ls}_c, as

$$p^{ls}_c = p^l - p^s$$ (68)

it can be seen from eqs 60 and 68 that

$$dp^{ls}_c = d\left(\gamma^{ls}\frac{dA^{ls}_{s,m}}{dV^{l}_m}\right).$$ (69)

Therefore, the capillary pressure of liquid water in a frozen porous medium can be calculated by

$$\int_0^{p^{ls}_c} dp^{ls}_c \equiv p^{ls}_c = \int_{T_0}^{T}\frac{S^{*l}_{m,H_2O} - S^{*s}_{m,H_2O}}{V^{*l}_{m,H_2O}}dT$$ (70)

or

$$p^{ls}_c = \int_{T_0}^{T}\frac{\Delta^l_s S^*_{m,H_2O}}{V^{*l}_{m,H_2O}}dT$$ (71)

where T_0 (K) is the freezing point of bulk liquid phase and $\Delta^l_s S^*_{m,H_2O}$ is the molar entropy of melting for pure water (J K^{-1} mol^{-1}).

Equation 77 is usually simplified by assuming that both V^{*l}_{m,H_2O} and $\Delta^l_s S^*_{m,H_2O}$ are constants, becoming

$$p^{ls}_c = \frac{\Delta^l_s S^*_{m,H_2O}}{V^{*l}_{m,H_2O}}t.$$ (72)

Equation 71 is often referred to as the generalized Clapeyron equation. The value of $\Delta^l_s S^*_{m,H_2O} / V^{*l}_{m,H_2O}$ can be calculated from physical measurements reported in the published literature. Since

$$\Delta^l_s S^*_{m,H_2O} = \frac{\Delta^l_s H^*_{m,H_2O}}{T^{l+s}}$$ (73)

the molar enthalpy of melting for water measured by Haida et al. (1974), 6006.8 J mol^{-1}, can be used. The value of V^{*l}_m at 0°C and atmospheric pressure is 18.0183 cm^3 mol^{-1} (Haar et al. 1984). The constant $\Delta^l_s S^*_{m,H_2O} / V^{*l}_{m,H_2O}$ therefore is 1.2205 MPa K^{-1}.

Following the suggestion of Koopmans and Miller (1966), the Clapeyron equation has long been applied to soil systems to estimate the matric potential of the liquid-water fraction of frozen soils.

This argument begins with the standard definition of capillary pressure, p_c (Pa):

$$p_c = p(\text{liquid soil water}) - p(\text{ambient atmospheric pressure})$$ (74)

which is related to matric potential by

$$\Psi = -\frac{p_c}{\rho g}$$ (75)

(Scheidegger 1974). A similar pressure, p_i, may be defined for frozen ground to express the pressure gradient across the ice/water interface in frozen ground

23

$$p_i = p(\text{liquid soil water}) - p(\text{ice}). \tag{76}$$

A term similar to matric potential can be defined for the pressure gradient across the ice/water interface in frozen ground:

$$\Psi_i = -\frac{p_i}{\rho g}. \tag{77}$$

If it is assumed that the volumetric content of soils for a given matric or supercooling potential is dependent solely on the ratios of pressure gradients to interfacial tensions,

$$\theta\left(\frac{\Psi}{\gamma_{wa}}\right) \approx \theta\left(\frac{\Psi_i}{\gamma_{iw}}\right) \tag{78}$$

then moisture-release and soil-freezing curves should be related by

$$\theta(\Psi) \approx \theta\left(-\frac{\gamma_{wa}}{\gamma_{iw}}\frac{p_i}{\rho_w^l g}\right). \tag{79}$$

The value of p_i as a function of temperature can be estimated by eq 72 and 73 if it is assumed that $p_i = \mathrm{d}p^{l+s}$ and $t - 0 = \mathrm{d}T$. The necessary data are

$$\gamma_{wa}\,(p = 0.1\ \text{MPa},\ t = 0.01°\text{C}) = 0.07564\ \text{N m}^{-1}\ \text{(Haar et al. 1984)}$$

$$\gamma_{iw}\,(p = 0.1\ \text{MPa},\ t = 0°\text{C}) = 0.033\ \text{N m}^{-1}\ \text{(Ketcham and Hobbs 1996)}$$

$$\Delta_s^l H_m^* = 343.2\ \text{J mol}^{-1}$$

$$V_m^{*l} = 18.018\ \text{cm}^3\ \text{mol}^{-1}$$

$$V_m^{*s} = 19.650\ \text{cm}^3\ \text{mol}^{-1}.$$

This implies that the pressure gradient across the ice/water interface changes with temperature according to

$$\frac{\mathrm{d}p^{l+s}}{\mathrm{d}T} = 7\,699\,\text{Pa K}^{-1} \equiv 7\,699\,\text{Pa °C}^{-1}. \tag{80}$$

Making the proper substitutions into eq 75,

$$\theta(\Psi) \approx \theta\left(-\frac{\gamma_{wa}}{\gamma_{iw}}\frac{\Delta_s^l H_m^*}{T_{fus}\Delta_s^l V_m^*}\frac{t}{\rho_w^l g}\right), \tag{81}$$

the following equation is derived:

$$\theta(\Psi) \approx \theta(ft) \tag{82}$$

where f is a constant approximately equal to -1.80 m H_2O °C^{-1}.

Changes in hydraulic conductivity with soil-water content

The relative-hydraulic-conductivity model proposed by van Genuchten (1980) has been adopted by many investigators. With some changes in notation, van Genuchten's model represents reduced water content, Θ (dimensionless), as a function of soil-water matric potential by:

$$\Theta = \left[\frac{1}{(\Psi\alpha)^\lambda + 1}\right]^{\frac{\lambda-1}{\lambda}} \tag{83}$$

24

where α (m^{-1}) and λ (dimensionless) are empirical parameters. The reduced water content is defined by

$$\Theta = \frac{(\theta - \theta_r)}{(\theta_s - \theta_r)} \tag{84}$$

where θ is the volumetric water content (dimensionless), and θ_s and θ_r are the saturated and residual volumetric water contents (dimensionless). The resulting empirical equations for volumetric water content are:

for unsaturated, unfrozen soils

$$\theta = \theta_r + (\theta_s - \theta_r)\left[\frac{1}{(\Psi\alpha)^\lambda + 1}\right]^{\frac{\lambda-1}{\lambda}} \tag{85}$$

and, by extension, for frozen, saturated soils:

$$\theta = \theta_r + (\theta_s - \theta_r)\left[\frac{1}{(f\!t\alpha)^\lambda + 1}\right]^{\frac{\lambda-1}{\lambda}}. \tag{86}$$

Similarly, the following equations may be used to calculate changes in relative permeability:

for unsaturated, unfrozen soils:

$$K_r(\Psi) = \frac{\left\{1 - \dfrac{(\alpha\psi)^{\lambda-1}}{\left[1+(\alpha\psi)^\lambda\right]^{\frac{\lambda-1}{\lambda}}}\right\}^2}{\left[1+(\alpha\Psi)^\lambda\right]^{\frac{\lambda-1}{2\lambda}}} \tag{87}$$

and for frozen, saturated soils:

$$K_r(t) = \frac{\left\{1 - \dfrac{(-\alpha f\!t)^{\lambda-1}}{\left[1+(-\alpha f\!t)^\lambda\right]^{\frac{\lambda-1}{\lambda}}}\right\}^2}{\left[1+(-\alpha f\!t)^\lambda\right]^{\frac{\lambda-1}{2\lambda}}}. \tag{88}$$

RESEARCH PRIORITIES

The literature survey presented here has revealed important gaps in scientific information that will impede the development of contaminant-transport models for cold regions:

1. The Pitzer model provides a powerful method by which to model the thermophysical behavior of electrolyte solutions below the freezing point of water. Unfortunately, there are few measurements with which to apply this tool. Physical–chemical properties of aqueous electrolyte solutions at subzero temperatures: isobaric heat capacities, molar volumes and viscosities, are needed.

2. A consistent thermodynamic treatment of the hydrostatics of liquid water in frozen porous media, a critical need, has yet to be developed.

25

3. Aside from permeability, the pressure-saturation relation for fluids in porous media is the most critical physical function for modeling the transport of fluids in variably saturated media. It has yet to be resolved entirely how temperature affects this relationship. A satisfactory understanding of the effect of temperature on soil retention curves for water and other liquids must be developed.

4. A co-ordinated research effort to determine the temperature effects on the physics of insoluble and sparingly soluble nonaqueous phase liquids in porous media should be pursued.

5. In frozen ground, the movement of solutes and water in response to osmotic and thermal gradients may be significant. Relations by which the transport of water, solutes, and nonaqueous phase liquids in response to thermal and osmotic gradients may be estimated reliably should be derived or developed.

CONCLUSION

A surprising number of cold-regions areas in the northern hemisphere are contaminated. There is a need to incorporate the fundamental physical, chemical, and hydrological processes that govern contaminant hydrology into the numerical models that are used to assist in the remediation of these sites. It is hoped this document assists in this process.

The physical and chemical processes that determine the fate of contaminants in cold regions are just now being understood comprehensively. As with any new area of understanding, this is a challenging process, but it is also an exciting area at the limits of our understanding of the dynamic behavior of complex, heterogeneous materials.

LITERATURE CITED

Archer, D.G. (1992) Thermodynamic properties of the NaCl + H$_2$O system, 2, Thermodynamic properties of NaCl(aq), NaCl · 2H$_2$O (cr), and phase equilibria. *Journal of Physical and Chemical Reference Data*, **21**: 793–829.

Atkins, P.W. (1990) *Physical Chemistry*. New York: W.H. Freeman and Co., 4th edition.

Bates, R.E. and M.A. Bilello (1966) Defining the cold regions of the Northern Hemisphere. USA Cold Regions Research and Engineering Laboratory, Technical Report 178.

Bureau International des Poids et Mesures (1984) *Le Système International d'Unités (SI)*. 6th edition. Sèvres, France: Bureau International des Poids et Mesures.

Callen, H.B. (1960) *Thermodynamics*. New York: John Wiley and Sons.

Constantz, J. (1991) Comparison of isothermal and isobaric water retention paths in non-swelling porous materials. *Water Resources Research*, **27**: 3165–3170.

Dorsey, N.E. (1940) *Properties of Ordinary Water Substance*. American Chemical Society. New York: Reinhold.

Everett, D.H. (1961) The thermodynamics of frost damage to porous solids. *Journal of the Chemical Society, Faraday Transactions*, **57**: 1541–1551.

Grigull, U., J. Straub, and P. Schiebener (1984) *Steam Tables in SI Units*. 3rd edition. Berlin: Springer-Verlag.

Guggenheim, E.A. (1957) *Thermodynamics: An Advanced Treatment for Chemists and Physicists*. 3rd edition. New York: Interscience Publishers.

Haar, L., J.S. Gallagher, and G.S. Kell (1984) *NBS/NRC Steam Tables*. New York: Hemisphere Publishing Corporation.

Hallett, J. (1963) The temperature dependence of the viscosity of supercooled water. *Proceedings, Physical Society (London)*, **82**: 1046.

Hare, D.E., and C.M. Sorenson (1987) The density of supercooled water, II. Bulk samples cooled to the homogeneous nuceation limit. *Journal of Chemical Physics*, **87**: 4840–4845.

Harned, H.S., and B.B. Owen (1958) *The Physical Chemistry of Electrolytic Solutions*. 3rd edition. New York: Reinhold for American Chemical Society.

Hill, P.G. (1990) A unified equation of state for H$_2$O. *Journal of Physical and Chemical Reference Data*, **19**: 1231–1274.

Huyakorn, P.S., and G.F. Pinder (1983) *Computational Methods in Subsurface Flow*. San Diego: Academic Press.

Jellinek, H.H.G. (1972) The ice interface. In *Water and Aqueous Solutions: Structure, Thermodynamics, and Transport Processes* (R.A. Horne, Ed.). New York: Wiley–Interscience.

Ketcham, W.M. and P.V. Hobbs (1969) An experimental determination of the surface energies of ice. *Philosophical Magazine,* **19**: 1161–1173.

Koopmans, R.W.R. and R.D. Miller (1966) Soil freezing and soil water characteristic curves. *Soil Science Society of America Proceedings,* **30**: 680–685.

Maier, C.G. and K.K. Kelley (1932) An equation for the representation of high-temperature heat content data. *Journal of the American Chemical Society,* **54**: 3243–3246.

Mangold, D.C. and C.-F. Tsang (1991) A summary of subsurface hydrological and hydrochemical models. *Reviews in Geophysica,* **29**: 51–79.

McGlashan, M.L. (1979) *Chemical Thermodynamics*. New York: Academic Press.

Nimmo, J.R. and E.E. Miller (1986) The temperature dependence of isothermal moisture vs. potential characteristics of soils. *Soil Science Society of America Journal,* **50**: 1105–1113.

Osipov, Y.A., B.V. Zheleznyi, and N.F. Bondarenko (1977) The shear viscosity of water supercooled to –35°C. *Zhurnal Fizicheskoi Khimii.,* **51**: 1264. [Translated to English in *Russian Journal of Physical Chemistry,* **51**(5): 748–749; 1977)].

Perfect, E., P.H. Groenevelt, and B.D. Kay (1989) Transport in frozen porous media. In *Transport Processes in Porous Media* (J. Bear and M.Y. Corapcioglu, Ed.). Boston: Kluwer Academic Publishers.

Philip, J.R., and D.A. de Vries (1957) Moisture movement in porous materials under temperature gradients. *EOS, Transactions of the American Geophysical Union,* **38**: 222–232.

Pitzer, K.S. (1991) Ion interaction approach, theory and data collection. In *Activity Coefficients in Electrolyte Solutions* (K.S. Pitzer, Ed.), 2nd edition. Boca Raton, Florida: CRC Press.

Robinson, R.A., and R.H. Stokes (1969) *Electrolyte Solutions.* 2nd edition. London: Butterworths.

Rowlinson, J.S. (1969) *Liquids and Liquid Mixtures.* 2nd edition. New York: Plenum Press.

Rowlinson, J.S., and B. Widom (1982) *Molecular Theory of Capillarity.* Oxford: Clarendon Press.

Scheidegger, A.E. (1974) *The Physics of Flow Through Porous Media.* 3rd edition. Toronto: University of Toronto Press.

Speedy, R.J. (1987) Thermodynamic properties of supercooled water at 1 atm. *Journal of Physical Chemistry,* **91**: 3354–3358.

Spencer, R.J., N. Møller, and J.H. Weare (1990) The prediction of mineral solubilites in natural waters, A chemical equilibrium model for the Na-K-Ca-Mg-Cl-SO_4-H_2O system at temperatures below 25°C. *Geochimica et Cosmochimica Acta,* **54**: 575–590.

Stokes, R.H. (1991) Thermodynamics of solutions. In *Activity Coefficients in Electrolyte Solutions* (K.S. Pitzer, Ed.), 2nd edition. Boca Raton, Florida: CRC Press.

Vand, V. (1948) Viscosity of solutions and suspensions, I. Theory. *Journal of Physical Chemistry,* **52**: 277–299.

van der Elsken, J.L. vanBoom, and A. Bot (1988) Hydrodynamic states in water below the temperature of the density maximum: The limit to supercooling. *Chemical Physics Letters,* **145**: 242–246.

van Genuchten, M.Th. (1980) A closed-form equation for predicting the hydraulic conductivity of unsaturated soils. *Soil Science Society of America Journal,* **44**: 892–898 .

Zheng, Q., D.J. Durben, G.H. Wolf, and C.A. Angell (1991) Liquids at large negative pressures: Water at the homogeneous nucleation limit. *Science,* **254**: 829–832.

27

REPORT DOCUMENTATION PAGE		Form Approved OMB No. 0704-0188

Public reporting burden for this collection of information is estimated to average 1 hour per response, including the time for reviewing instructions, searching existing data sources, gathering and maintaining the data needed, and completing and reviewing this collection of information. Send comments regarding this burden estimate or any other aspect of this collection of information, including suggestions for reducing this burden to Department of Defense, Washington Headquarters Services, Directorate for Information Operations and Reports (0704-0188), 1215 Jefferson Davis Highway, Suite 1204, Arlington, VA 22202-4302. Respondents should be aware that notwithstanding any other provision of law, no person shall be subject to any penalty for failing to comply with a collection of information if it does not display a currently valid OMB control number. PLEASE DO NOT RETURN YOUR FORM TO THE ABOVE ADDRESS.

1. REPORT DATE (DD-MM-YY) December 2000	2. REPORT TYPE Technical Report	3. DATES COVERED (From - To)

4. TITLE AND SUBTITLE Physical and Chemical Factors Affecting Contaminant Hydrology in Cold Environments	5a. CONTRACT NUMBER
	5b. GRANT NUMBER
	5c. PROGRAM ELEMENT NUMBER
6. AUTHOR(S) Steven A. Grant	5d. PROJECT NUMBER
	5e. TASK NUMBER
	5f. WORK UNIT NUMBER

7. PERFORMING ORGANIZATION NAME(S) AND ADDRESS(ES) U.S. Army Cold Regions Research and Engineering Laboratory 72 Lyme Road Hanover, New Hampshire 03755-1290	8. PERFORMING ORGANIZATION REPORT NUMBER ERDC/CRREL TR-00-21

9. SPONSORING/MONITORING AGENCY NAME(S) AND ADDRESS(ES) U.S. Army Waterways Experiment Station, Office of the Chief of Engineers, and Strategic Environmental Research and Development Program	10. SPONSOR / MONITOR'S ACRONYM(S)
	11. SPONSOR / MONITOR'S REPORT NUMBER(S)

12. DISTRIBUTION / AVAILABILITY STATEMENT

Approved for public release; distribution is unlimited.

Available from NTIS, Springfield, Virginia 22161.

13. SUPPLEMENTARY NOTES

14. ABSTRACT

This report surveys some of the physical and chemical effects of cold temperatures that should be considered when developing a contaminant-transport model. This discussion begins with a working definition of cold regions for the purpose of contaminant hydrology modeling: an area with appreciable frozen ground and with a substantial fraction of the annual precipitation falling as snow. The chemical thermodynamics of geochemical solutions below 0°C is then reviewed. Particular attention is placed on the physical–chemical properties of ice and liquid water at subzero temperatures. Finally, models that estimate the liquid water content and hydraulic conductivity of frozen ground are discussed.

15. SUBJECT TERMS

Cold regions	Groundwater
Geochemistry	Permafrost

16. SECURITY CLASSIFICATION OF:			17. LIMITATION OF ABSTRACT	18. NUMBER OF PAGES	19a. NAME OF RESPONSIBLE PERSON
a. REPORT	b. ABSTRACT	c. THIS PAGE			
U	U	U	U	29	19b. TELEPHONE NUMBER (include area code)

Standard Form 298 (Rev. 8-98)
Prescribed by ANSI Std. 239.18